Electrical conductivity of a strongly correlated aluminium plasma

2003 J. Phys. A: Math. Gen. 36 6033

(http://iopscience.iop.org/0305-4470/36/22/327)

INSTITUTE OF PHYSICS PUBLISHING JOURNAL OF PHYSICS A: MATHEMATICAL AND GENERAL

J. Phys. A: Math. Gen. **36** (2003) 6033–6039 PII: S0305-4470(03)54648-0

Electrical conductivity of a strongly correlated aluminium plasma

Vanina Recoules, Jean Clérouin, P Renaudin, P Noiret and Gilles Zérah

Département de Physique Théorique et Appliquée, CEA/DAM Île-de-France, BP12, 91680 Bruyères-le-Châtel Cedex, France

E-mail: vanina.recoules@cea.fr

Received 25 November 2002
Published 22 May 2003
Online at stacks.iop.org/JPhysA/36/6033

Abstract

We present theoretical estimations of the electrical conductivity of a warm expanded aluminium plasma ($\rho = 0.3$ g cm^{-3}). Our calculations are carried out in the framework of density functional theory and the local density approximation. Ionic configurations were determined by *ab initio* molecular dynamics simulations, from which the conductivity was computed using the Kubo–Greenwood formula. Theoretical results were validated in the dense coupled regime ($\rho = 2$ g cm^{-3}) against previously published experimental results. For the low-density regime, the result is compared to experiments obtained in our laboratory in an isochoric closed-vessel designed to confine electrical plasma discharges up to 1.5 GPa. In this regime we show that the usual Drude model is no longer relevant and that the electrical conductivity is driven by the optical properties.

PACS numbers: 52.25.−b, 52.65.−y, 52.50.−b, 52.70.−m

1. Introduction

Many models for computing electrical conductivity have been developed to account for strong coupling (SC) and partial degeneracy effects [1, 2]. Most of these rely on the Ziman theory [3, 4], which requires, as an input function, knowledge of the ionic structure factor. In this regime, the interactions between ions are screened by the electronic polarization and up to now there has been no correct model to account for non-linear screening. *Ab initio* molecular dynamics is ideally suited for this type of problem, precisely because no adjustable parameters or empirical inter-ionic potentials are needed. The energetics of the system and the forces on the ions are calculated by first-principle methods, which make the subsequent ionic structure consistent with the degeneracy of the electrons. This method has been successfully used on liquids [5–8] and is applied in this paper to a theoretical calculation of the electrical conductivity of expanded aluminium at low density

($\rho = 0.3$ g cm^{-3}). This regime corresponds to recent experimental measurements obtained in an isochoric plasma closed-vessel (EPI) designed to confine electrical plasma discharges up to 1.5 GPa.

The experiment is described at length in [9, 10]. In the EPI device, the plasma is kept in a constant volume channel during a slow electrical discharge (250 μs). The confinement is realized by the mechanical properties of the chamber and the plasma phase can be considered almost isochoric. This allows direct measurements, in the course of the electrical discharge, of mass density, input energy and electrical conductivity without any external model [9]. In most experiments on aluminium, temperature is not directly measured but deduced from measurements of energy input, or measured spectroscopically [11, 12]. We have chosen to plot electrical conductivity versus internal energy variation, which is unusual. This is a pertinent representation which avoids the need of an external model to compare experimental and theoretical results.

Such a dilute metallic system is a new field of application for *ab initio* simulations and computation of the electrical conductivity. In order to verify our implementation of the method, we first present results in the dense degenerate regime ($\rho = 2$ g cm^{-3}) where experimental results and computational estimations are available showing the validity of the Drude model at high density.

2. *Ab initio* calculations

The most general formulation for computing the electrical conductivity is given by the Kubo–Greenwood formulation in which no particular assumptions are made on the ionic structure or on the electron–ion interactions. The real part of the optical conductivity $\sigma(\omega)$ is given by

$$\sigma(\omega) = \frac{2\pi e^2}{3\omega}\frac{1}{\Omega}\sum_{\boldsymbol{k}} W(\boldsymbol{k}) \sum_{n,m} \left(f_n^{\boldsymbol{k}} - f_m^{\boldsymbol{k}}\right)\frac{1}{(2\pi^2)} \times \left|\left\langle \psi_n^{\boldsymbol{k}} \middle| \hat{v} \middle| \psi_m^{\boldsymbol{k}} \right\rangle\right|^2 \delta\left(E_m^{\boldsymbol{k}} - E_n^{\boldsymbol{k}} - \hbar\omega\right) \qquad (1)$$

where ω is the frequency, e is the electronic charge, ψ_n and E_n are the electronic eigenstates and eigenvalues for the electronic state n at a given $\boldsymbol{k}$-point in the Brillouin zone, f_n is the Fermi distribution function, and $\hat{\boldsymbol{v}}$ is the velocity operator. Calculations of the eigenstates and eigenvalues are made in the framework of density functional theory. $W(\boldsymbol{k})$ is the $\boldsymbol{k}$-point weight in the Brillouin zone using the Monkhorst–Pack scheme. In most publications using the Kubo–Greenwood formalism [6, 7, 13], the velocity operator $\hat{\boldsymbol{v}}$ is expressed as the momentum operator $\frac{\hat{\boldsymbol{p}}}{m}$. This is correct if the Hamiltonian contains only local potential. In our case, nonlocal pseudo-potentials are used and this equivalence is no longer valid. Then, we compute the real velocity matrix elements $\left\langle \psi_n^{\boldsymbol{k}} \middle| \hat{v} \middle| \psi_m^{\boldsymbol{k}} \right\rangle$. Technical details of the computation of matrix elements can be found in [14, 15]. The δ function can be resolved by using a Gaussian regularization. The dc electrical conductivity σ_{dc} computation is obtained by extrapolating optical conductivity to $\omega = 0$.

All of our simulations use constant density and volume. We use a finite sample in a basic cubic reference cell, with a finite number of electrons. We also invoke periodic boundary conditions. The simulation of periodic systems introduces the question of Brillouin zone sampling. Methods have been devised for obtaining very accurate approximations to the electronic potential and the contribution to the total energy from electronic orbitals by calculating the electronic states at special $\boldsymbol{k}$-points in the Brillouin zone (BZ). For large disordered systems, this constraint becomes less compelling and simulations at the Γ point can be used. The electrical conductivity and, more generally, optical properties are very sensitive to a detailed description of the electronic density. In particular, a correct BZ sampling is necessary to obtain accurate results. This observation has led us to use a two-step procedure.

In a first step, the ionic structure is generated with the *ab initio* code, VASP, developed at the Technical University of Vienna [16], in which ion–electron interactions are described with Vanderbilt ultra-soft pseudo-potentials [17]. The Perdew and Wang parametrization of the generalized gradient approximation [18] is used for the exchange and correlation potential. The generation of atomic structures is carried out at the Γ point and is performed for 32 or 108 atoms for 300 to 500 time steps of 2 fs after equilibration without a thermostat (pure microcanonical). We consider electronic states occupied down to 10^{-6}.

In a second step, for selected statistically independent atomic configurations, a self-consistent ground-state calculation is performed with the ABINIT code [19, 20] to obtain the detailed electronic structure. The electronic calculation is performed in the local density approximation (LDA) with the Ceperley–Adler [21] exchange-correlation energy as parametrized by Perdew and Wang [22]. The pseudopotential used in our work is generated by the method of Troullier–Martins [23]: 3*s* and 3*p* states are treated as valence electrons and we use a *d* non-local part. Orbitals are expanded in plane waves up to a cut-off of 12 Ry. The BZ was sampled with the Monkhorst–Pack scheme [24] and convergence in $\boldsymbol{k}$-vectors was tested. We find that for simulations with 108 atoms, convergence is reached with the use of four special $\boldsymbol{k}$-points. For high density, between 250 (for $T = 1000$ K) and 500 (for $T = 14\,500$ K) orbitals are considered for a 108-atom cubic cell. For low density, between 300 and 500 orbitals are considered for a 32-atom cubic cell.

3. Results

3.1. Dense degenerate regime ($\rho = 2$ g cm^{-3})

As mentioned in section 2, we first performed *ab initio* simulations with the VASP code using 108 particles at three temperatures: 1000, 5000 and 14 500 K. Trajectories were generated for 500 time steps of 2 fs at the Γ point.

In order to check our implementation of the method, we computed the electrical conductivity at a density of 2 g cm^{-3} representative of expanded liquid aluminium. From the molecular dynamics simulations performed at the Γ point, the electronic structure has been computed for five statistically independent configurations with four $\boldsymbol{k}$-points. As an example, the density of occupied states (DOS) and the optical conductivity at 14 500 K are presented in figure 1. The shape of the DOS and of the optical conductivity does not change with temperature [10]. As expected in this regime, the DOS exhibits the usual free-electron-like behaviour. There is neither a gap nor minimum near the Fermi level. The Drude formula

$$\sigma(\omega) = \frac{\sigma_{\mathrm{dc}}}{1 + \omega^2\tau^2} \tag{2}$$

where τ is the relaxation time, accurately reproduces the optical conductivity $\sigma(\omega)$ (figure 1(*b*)) confirming the metallic character of aluminium at $\rho = 2$ g cm^{-3}. Using this fit, the zero-frequency limit yields the dc conductivity. As shown in figure 2, we found an excellent agreement with previous theoretical calculations [6, 25] and experimental measurements [26–28].

3.2. Partially degenerate regime ($\rho = 0.3$ g cm^{-3})

Using the same procedure, we generated ionic configurations representative of the plasma created in the EPI ($\rho = 0.3$ g cm^{-3}). It must be noted that such a small density is much more demanding of computer resources than the previous case because of a larger simulation box and, consequently, the number of plane waves to be computed. This is why microcanonical

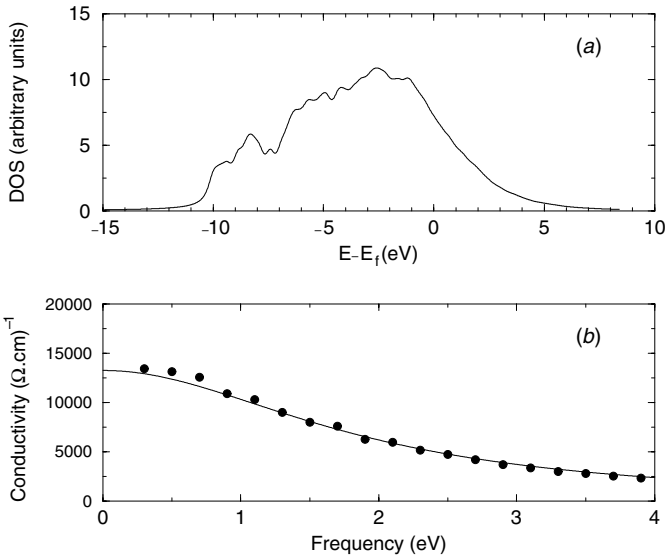

Figure 1. Density of states (*a*) and optical conductivities (*b*) at $T = 14\,500$ K and $\rho = 2$ g cm^{-3}. The full line in (*b*) is the Drude fit given by equation (2).

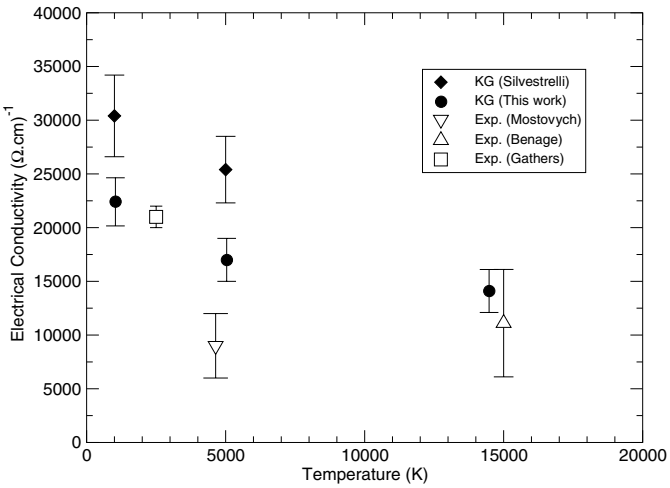

Figure 2. Electrical dc conductivity versus temperature at $\rho = 2$ g cm^{-3}. Our model (full circles) is compared with simulations of Silvestrelli (full diamond, [6]) and with the experiments of [28] (square), [26] (up triangle) and [27] (down triangle).

simulations are performed for only 32 atoms, for 300 time steps after equilibration for $T = 7600$, 11 700 and 16 400 K. The evaluation of internal energy variation using quantum molecular dynamics allows a direct comparison against the experimental points obtained in the EPI. As in the previous case, the optical analysis is derived afterwards from selected ionic configurations.

The DOS and the optical conductivity are shown in figure 3. The general shape of the DOS and of the optical conductivity does not change with temperature [10]. We no longer

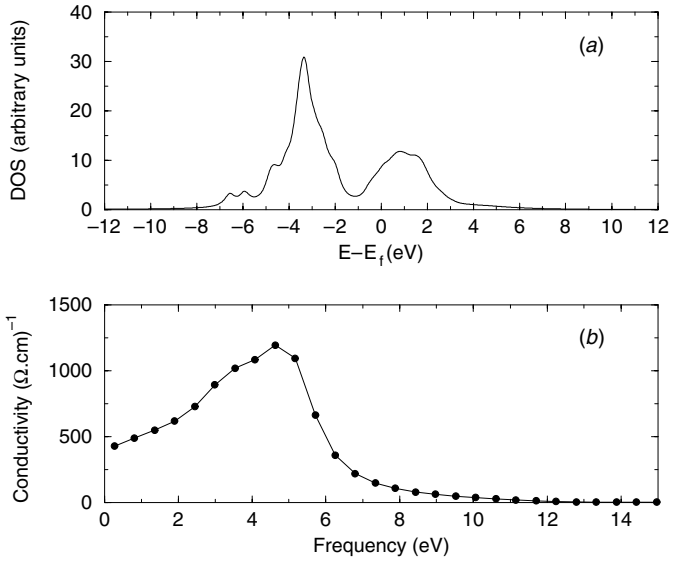

Figure 3. Density of states (*a*) and optical conductivities (*b*) at $\rho = 0.3$ g cm^{-3} and $T = 16\,400$ K.

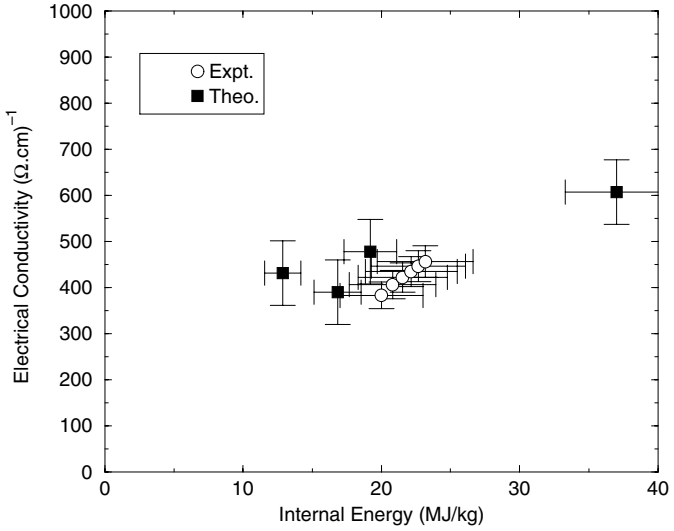

Figure 4. Electrical dc conductivity (full circles) versus internal energy at $\rho = 0.3$ g cm^{-3} compared with our experimental data (open circles).

observe a free-electron-like form and a structure appears in the DOS. The band centred on ~ -3 eV is due to the 3*s* electrons and shoulder around ~ -2 eV due to the 3*p* electrons.

Clearly, optical conductivities, plotted versus frequency in figure 3(*b*), are no longer characteristic of a simple free-electron Drude metal but are more reminiscent of non-metallic systems [5, 13]. In view of the difference in the DOS between the two densities, it is not surprising to find that electrical conductivity changes dramatically. The peak around 5 eV can be attributed to the transitions between the occupied bands at ~ 3 eV below the Fermi level

of 3*s* character and the partially occupied states with energies ∼2 eV above the Fermi level of 3*p* character.

The resulting experimental and theoretical electrical conductivities are plotted as a function of the internal energy in figure 4 and are compared to the experiments. The vertical error bars on the experimental points indicate the uncertainty in the conductivity resulting from voltage, current and geometry measurements. The uncertainty in the internal energy is assumed to be equal to the uncertainty in the input electrical energy, i.e. 15%. For the theoretical conductivities, the extrapolation to zero frequency is much more difficult due to the statistical noise of the optical spectra at low frequency leading to large errors bars in figure 3. The extrapolation is carried out using a cubic regression on the four first points. The order of magnitude of the conductivity is characteristic of a semiconductor in accordance with the shape of the optical conductivity. The computed electrical conductivity agrees well with the experimental conductivity.

4. Conclusion

We have computed the electrical conductivity of an aluminium plasma at low density $\rho = 0.3$ g cm^{-3} using *ab initio* molecular dynamics and Kubo–Greenwood formulation. The predicted conductivities are in very close agreement with recent experimental data obtained with the EPI facility and are showing a dramatic change from a Drude behaviour at high density, to a semiconductor-like behaviour at low density.

Acknowledgments

We gratefully acknowledge S Bernard for supplying the pseudopotential, M Torrent, F Jollet, X Gonze and S Mazevet for useful discussions, and B Loffredo and M Sonnaert for their technical assistance during the course of this work.

References

[1] Kuhlbrodt S and Redmer R 2000 Transport coefficients for dense metal plasmas *Phys. Rev.* E **62** 7191
[2] Perrot F and Dharma-Wardana M W C 1995 Equation of state and transport properties of an interacting multispecies plasma: Application to a multiply ionized Al plasma *Phys. Rev.* E **62** 5352
[3] Ziman J M 1961 *Phil. Mag.* **6** 1013
[4] Evans R, Greenwood D A and Lyod P 1971 *Phys. Lett.* A **35** 57
[5] Collins L A, Bickham S R, Kress J D, Mazevet S, Lenosky T J, Troullier N J and Windl W 2001 Dynamical and optical properties of warm dense hydrogen *Phys. Rev.* B **63** 184110
[6] Silvestrelli P L 1999 No evidence for a metal–insulator transition in dense hot aluminum: A first-principles study *Phys. Rev.* B **60** 16382
[7] Holender J M, Gillan M J, Payne M C and Simpson A D 1995 Static, dynamic, and electronic properties of liquid gallium studied by first-principles simulation *Phys. Rev.* B **52** 967
[8] Galli G, Martin R M, Car R and Parrinello M 1989 Carbon: the nature of the liquid state *Phys. Rev. Lett.* **63** 988
[9] Renaudin P, Blancard C, Faussurier G and Noiret P 2002 Equation of state and electrical resistivity measurements of warm dense aluminum and titanium plasmas *Phys. Rev. Lett.* **88** 215001
[10] Recoules V, Renaudin P, Clérouin J, Noiret P and Zérah G 2002 Electrical conductivity of hot expanded aluminum: Experimental measurements and *ab initio* calculations *Phys. Rev.* E **66** 056412
[11] De Silva A W and Katsouros J D 1998 Electrical conductivity of dense copper and aluminum plasmas *Phys. Rev.* E **57** 5945
[12] Krisch I and Kunze H J 1998 Measurements of electrical conductivity and the mean ionization state of non-ideal aluminium plasma *Phys. Rev.* E **58** 6557
[13] Fois E, Selloni A and Parrinello M 1989 Approach to metallic behavior in metal-molten-salt solutions *Phys. Rev.* B **39** 4812

[14] Gonze X 1997 First-principles responses of solids to atomic displacements and homogenous electric fields: implementation of a conjugate-gradient algorithm *Phys. Rev.* B **55** 10337
[15] Gonze X and Lee C 1997 Dynamicals matrices, born effective charges, dielectric permittivity tensors and interatomics force constants from density functional perturbation theory *Phys. Rev.* B **55** 10355
[16] Kresse G and Hafner J 1993 *Ab initio* molecular dynamics for liquid metals *Phys. Rev.* B **47** 558
[17] Vanderbilt D 1990 Ultrasoft pseudopotentials *Phys. Rev.* B **41** 7892
[18] Perdew J P 1991 *Electronic Structure of Solids*. (Berlin: Akademie Verlag)
[19] Gonze X, Beuken J-M, Caracas R, Dutraux F, Fuchs M, Rignanese G-M, Sindic L, Verstraete M, Zerah G, Jollet F, Torrent M, Roy A, Mikami M, Ghosez Ph, Raty J-Y and Allan D C 2002 First-principles computation of material properties: the abinit software project *Comput. Mater. Sci.* **25** 478
[20] Payne M C, Teter M P, Allan D C, Arias T A and Joannopoulos J D 1992 Iterative minimization techniques for *ab initio* total energy calculations: molecular dynamics and conjugate gradients *Rev. Mod. Phys.* **64** 1045
[21] Ceperley D M and Alder B J 1980 Ground state of the electron gas by stochastic method *Phys. Rev. Lett.* **45** 566
[22] Perdew J P and Wang Y 1986 Accurate and simple density functional for the electronic exchange energy: generalized gradient approximation *Phys Rev.* B **33** 8800
[23] Troullier N and Martins J L 1991 Efficient pseudopotentials for plane-wave calculations *Phys. Rev.* B **43** 1993
[24] Monkhorst H J and Pack J D 1976 Special points for Brillouin-zone integrations *Phys. Rev.* B **13** 5188
[25] Desjarlais M P, Kress J D and Collins L A 2002 Electrical conductivity for warm, dense aluminium plasmas and liquids *Phys. Rev.* E **66** 025401
[26] Benage J F, Shanahan W R and Murillo M S 1999 Electrical resistivity measurements of hot dense aluminum *Phys. Rev. Lett.* **83** 2953
[27] Mostovych A N and Chan Y 1997 Reflective probing of the electrical conductivity of hot aluminum in the solid, liquid and plasma phases *Phys. Rev. Lett.* **79** 5094
[28] Gathers G R 1983 Conductivity of aluminum liquid *Int. J. Thermophys.* **4** 209